Cryogenic vacuum considerations for future gravitational wave detectors

L. Spallino,[1,*] M. Angelucci,[1] A. Pasqualetti,[2] K. Battes,[3] C. Day,[3] S. Grohmann,[3] E. Majorana,[4] F. Ricci,[4] and R. Cimino[1,†]

[1]*LNF-INFN, Via E.Fermi 40, 00044 Frascati (Rome), Italy*
[2]*European Gravitational Observatory (EGO), 56021 Cascina (Pisa), Italy*
[3]*Karlsruhe Institute of Technology (KIT), Hermann-von-Helmholtz-Platz 1, 76344, Eggenstein-Leopoldshafen, Germany*
[4]*Dipartimento di Fisica, Universitá degli Studi di Roma "La Sapienza," Roma, Italy*

(Received 25 May 2021; accepted 20 July 2021; published 2 September 2021)

In recent years, gravitational wave observatories have conquered the world science scene due to their unprecedented capability to observe astrophysical signals. Those first observations opened up multimessenger astronomy and called for a tremendous R&D effort to improve the sensitivity of future detectors. One of the many issues to be solved, not to affect the desired sensitivity, is the noise induced by the use of room temperature mirrors, especially for the low-frequency detection range. The use of cryogenic mirrors to reduce such a noise source has been individuated as a viable solution to obtain the desired sensitivity at low frequency. Cryogenically cooled mirrors, routinely operating at 10 K, present a number of extraordinary challenges, one being the cryogenic vacuum system hosting the cold mirrors. Gases composing the residual vacuum will tend to cryosorb and build a contaminant ice layer ("frost") on the mirror surface. Depending on such ice layer thickness, various unwanted detrimental effects may occur affecting mirror performances. This paper analyzes the consequences of hosting a cryogenically cooled mirror in a vacuum system and sets new limits for an acceptable operating pressure to avoid frost formation in a given period of continuous data taking. Since ice formation can be reduced but not avoided, we analyze potential mitigation methods to cure such a phenomenon. Thermal and nonthermal methods are analyzed and compared. Electron stimulated desorption is also considered as an alternative method to desorb the ice layer on mirrors. Finally, we briefly discuss further studies needed to validate the various methods with special care on their effects on the mirror perfection and optical properties.

DOI: 10.1103/PhysRevD.104.062001

I. INTRODUCTION

From the first detection of gravitational waves (GWs) in 2015 [1], the interferometry detection method has been established as an extremely powerful tool to significantly enrich multimessenger astrophysics for years to come. In the ongoing and future research, it is of paramount importance to reduce undesired noise that can limit the sensitivity of gravitational interferometers and, hence, their physical reach. Higher sensitivities are indeed foreseen to be essential to reveal the nature of GWs [2], the evolution of black holes [3], and the Hubble constant. Among other noise sources, coating thermal noise (CTN) is one of the limiting factors in the presently operational interferometers. All the advanced observatories will reach their design sensitivity if CTN is under control and opportunely mitigated [4–6]. CTN is intrinsic to mirrors, and its amplitude spectral density, to which a gravitational wave detector is sensitive, is proportional to $\sqrt{T}$. For this reason, cooling the mirrors is a very promising way to reduce CTN and, therefore, to improve sensitivity [7], especially in the low-frequency range. This approach is already foreseen at the Japanese KAGRA detector [8–10], which is currently under commissioning, for the low-frequency detector of the planned Einstein Telescope (ET LF) [11–13] and for the American Cosmic Explorer [14]. Cooling and running a suspended mirror of up to 200 kg at temperatures as low as 10 K presents a number of extraordinary technological challenges that will attract an enormous research and development effort in the coming years. Among other issues, a cryogenically cooled mirror will inevitably undergo the formation of a contaminant cryosorbed layer that could seriously affect mirror optical performances. Indeed, as reported in Refs. [15–17], the cryocooled mirrors at the KAGRA GW detector undergo a decrease in reflectivity due to ice growth. Its formation is induced by molecules both residual in the mirror vessel and moving from the warm laser beam transfer line. In those works, the authors assume water molecules as the dominant source of

*Luisa.Spallino@lnf.infn.it
†Roberto.Cimino@lnf.infn.it

frosting, since the experimental data in Ref. [16] were measured in a water-rich test setup. It is not clear if water may or may not be the dominant constituent of frosting in the different operational runs of KAGRA. This will depend on the actual details of the KAGRA vacuum system and on the adopted pumping strategy. In any case, adsorbed molecules will build up an adlayer on top of the cold mirror coating and not only affect mirror optical properties [16], but also contribute to CTN [6]. The reflectivity of the mirror in KAGRA was expected and observed to change periodically as the ice layer grew through multiples of quarter wavelengths in optical thickness. In addition, a long-term reflectivity decrease is predicted and observed due to the optical absorption of the cryosorbed adlayer. As a result, the circulating laser power in the interferometer will steadily decrease over time, and its value will also oscillate as due to the periodic reflectivity change. Depending on the wavelength at which the coating is designed to be reflective, reflectivity oscillations are expected to occur already after ≈300 nm of ice grown on the surface and are expected to have a significant impact on the detector sensitivity when the ice thickness is above one micron. Much more worrying are the results presented by a recent work from Tanioka, Hasegawa, and Aso [17]. They theoretically estimate the optical loss by the molecular layer in a cryogenically operated gravitational wave detector. The authors estimate the absorption induced by the overlayer from the predicted optical loss. Such power absorption is indeed quite significant and has the potential to prevent stable cryogenic operation. For the discussed case of KAGRA, a few tens of nanometers of ice adlayer can absorb enough power to generate an additional heat load to the test masses equivalent to the available thermal budget. Any increase in the adlayer thickness will then increase the set temperature of the test mass [17]. Tanioka, Hasegawa, and Aso's estimate for the ET detectors is even more severe. Already, a few nanometers of ice coverage can absorb more than the 100 mW cooling budget predicted to keep the mirrors at the foreseen temperature of 10 K. A growing layer will induce more and more heat load on the test masses and drift their temperature in an uncontrolled way. All these effects clearly deserve further studies, since, indeed, they can severely affect the sensitivity of the new GW detectors. In any case, it is clear that the growth of an unwanted adlayer on mirrors must be avoided and/or efficiently mitigated.

This paper presents a simple analysis on the way one can estimate the ice growth layer on the mirrors and analyses a number of potential methods to passively or actively mitigate such growth.

II. CRYOGENIC VACUUM CONSIDERATION

The understanding of complex and/or large vacuum systems operating at cryogenic temperatures requires a specific knowledge of vacuum science at such temperatures. In fact, at cryogenic temperatures, the sojourn time of some molecular species is significantly increased. Sticking probabilities, capture factor, and thermal transpiration concepts are then used to characterize the adlayer formation mechanism [18,19]. At cryogenic temperature, a gas load into a vacuum system turns into an increase of the surface coverage due to the attractive van der Waals forces and its associated vapor pressure. Here, we refer to the relevant literature on those topics and limit to giving some basic information in order to estimate the vacuum requirements to inhibit, if possible at all, or anyway limit the growth of any significant thickness of an ice adlayer on mirrors in cryogenic gravitational interferometers.

As said, there are two main sources of contaminants that can be adsorbed to the mirror surface. One derives from the residual gas content of the ultrahigh vacuum (UHV) chamber where the mirror is contained; the other comes from the gas drifting from the room temperature (RT) section of the interferometer along with the laser radiation. Hereafter, we first analyse the type and quantities of gases one needs to consider.

A. Pressures in cryogenic environment

It is not good practice to install vacuum gauges and quadrupole mass spectrometers (QMS) in a cryogenic environment. All such measuring devices use hot filament for ionizing the residual gases, and, if installed close to a low-temperature system, they may induce unwanted additional heat load on it. In general, and in the experiments discussed in Ref. [16], the vacuum measurements are usually made by vacuum gauges located in a room temperature vacuum vessel in connection to the cryosystem. If this is the case, a thermal transpiration correction must be applied (the Knudsen relationship) to the pressure readings under free molecular flow conditions [18–20]. When two vessels at two different temperatures T_1 and T_2 communicate by a small aperture, the collision rate is conserved when the steady state is established. By equating the fluxes, since the mean velocity scales with T, it is

$$p_1/p_2 = \sqrt{T_1}/\sqrt{T_2}. \tag{1}$$

In practice, from Eq. (1), when the pressure p_1 is measured at room temperature $T_1 = 300$ K, the pressure p_2 inside a vacuum vessel at $T_2 = 4.2$ K (liquid helium) or at $T_2 = 77$ K (liquid nitrogen) is $p_2 \sim p_1/8$ or $p_2 \sim p_1/2$, respectively. Note that the T mentioned here is the one related to the molecule velocity and represents the mean temperature of a gas in thermal equilibrium with its cryogenic vessel. So, this reasoning applies when a fully closed cryogenic system is connected to a RT one. In gravitational wave interferometers, not only is the mirror vessel generally a big tower of approximately 10 m^3 internal volume, but it also has quite a complex design. It will be formed by uncooled components, that will contribute to the base pressure by RT desorption, and by some cryogenic thermal screens around

the cooled mirror, whose face must be free, of course, to look at the impinging laser beam. This may affect the equilibrium temperature of the molecules close to this surface and, hence, will reduce the pressure scaling factor when thermal transpiration correction is applied to the real system. To avoid such uncertainties, for more detailed vacuum simulations, it is current practice to directly indicate gas densities rather than pressure values for cryogenic systems. Here, for simplicity, we continue considering the pressure p as the relevant parameter.

B. Cryosorbed gases

Residual gas in vacuum will stick to the cold, flat, mirror surface depending on the gas species and pressure values. In the following, let us assume, for simplicity and to be conservative, a sticking coefficient close to unity. This assumption is indeed very reasonable and will not be discussed any further [18–22]. To understand what types of gases will be forming the adlayer on the mirrors, one can look at Fig. 1 from Ref. [23]. Figure 1 shows an instructive plot, on which generations of cryovacuum users had formed, reporting the saturated vapor pressures of the most common gases forming the residual vacuum of a clean UHV system. The saturated vapor pressure of a single gas species is the pressure of this gas over its liquid or its solid phase, i.e., the P-T values at which a gas is condensed as a multilayer. The pressures, to be corrected from the aforementioned thermal transpiration, are at room temperature [18–20,24]. Figure 1 indicates that, below 20 K, the saturated vapor pressures of most of the gases is below 10^{-12} mbar. Therefore, large quantities of such gases will be cryosorbed on the mirror surface if its surface is ≈20 K or below. If the mirror surface is at temperatures between 25 and 120–150 K, water ice will eventually grow on it. Its thickness and the time to affect the mirror properties depends not only on the detailed vacuum composition of the tower, but also on the vacuum seen by the mirror during cooling down and, inevitably, on the gas flow from the room temperature high-conductivity vacuum tubes to the cold surfaces.

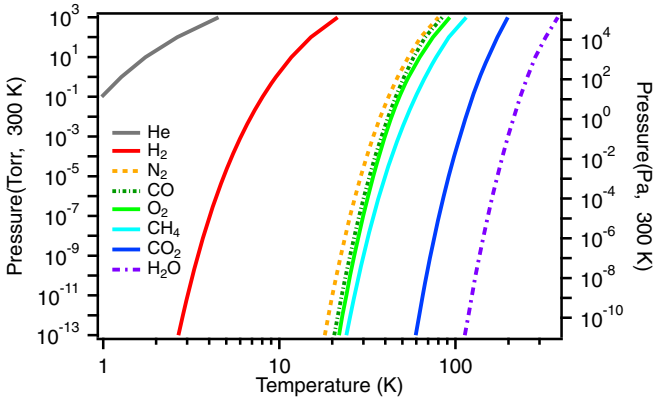

FIG. 1. Saturated vapor pressure of some of the most common gases forming the residual vacuum of a clean UHV system [23].

Here, we ignore the known possibility of a condensed gas to trap a noncondensable gas with a lower vapor pressure. This effect, called cryotrapping, may add to the cryosorbed layer some H_2 and He molecules that may influence its optical quality.

C. Gas composition versus total pressure

From the previous subsection, it is clear that, rather than the total pressure (i.e., the total number of molecules contained in the vacuum vessel), we should be interested in partial pressure values (i.e., the number of specific H_2O, CO, CO_2, N_2, etc., molecules contained in the vacuum vessel). Gas-specific partial pressures can indeed be measured by a calibrated QMS [25]. This instrument will give the percentage composition, i.e., the residual gas analysis (RGA), contributing to the total pressure. For absolute readings, the QMS usually being placed in a room temperature vacuum vessel connected to the cryogenic system, not only do we need to consider the already discussed thermal transpiration correction, but a careful calibration with known quantities of a given gas must be conducted [26] following standard procedures (ISO/TS 20175:2018-04).

There is no easy and universal scaling between the total pressure value and the single-gas composition, since, in standard UHV equipment, the detailed composition of the residual gas depends on various aspects, ranging from humidity in the atmosphere to contaminants (or, eventually, pollution) present in the vacuum systems and on the way the system is pumped and on the vessel treatment. For the sake of discussion here, we show the normalized ion currents approximately reflecting the mass species composition of a stainless steel (AISI 304), before and after vessel thermal treatment. Thermal treatment of a vacuum system, usually called bakeout, implies heating all the vessel surfaces at a temperature as high as possible (in the range $100 - 400\,°C$) for a long period (typically going from 24 h to a few days) during standard pump down. A bakeout at higher temperature may additionally decrease the H_2O content of the residual gases [27], confirming that detailed RGA measurements should, therefore, be performed on each system and publications should include such details for referencing.

The desorption process is characterized by the so-called sojourn time τ, the mean lifetime of a molecule on a surface. It is known [18,19,25] that the higher the temperature of the surface, the shorter the sojourn time. A molecule that has a short sojourn time on the vessel wall has higher probability to be pumped away by the active pumping system. This is finally the reason why it is common practice to bakeout a vacuum system. As seen in Fig. 2 (top panel), the residual gas composition of an unbaked vacuum system ($p \approx 4 \times 10^{-9}$ mbar) is dominated by water. At room temperature, the sojourn time is

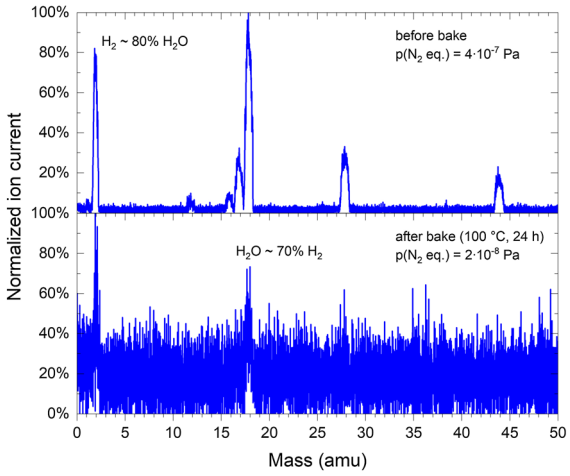

FIG. 2. Residual gas analysis, as measured with a QMS in the case of a clean UHV system prior (top panel) and after an *in situ* bakeout (bottom panel) at 100 °C for 24 h.

100 h for water, 3 min for hydrogen, and more than 6 months for carbon monoxide. Increasing the temperature of the vacuum vessel above 100 °C reduces the H_2O sojourn time to about a minute and, hence, strongly reduces the surface coverage and also the outgassing rate of water at room temperature after bakeout. As can be seen in Fig. 2 (bottom panel), the bakeout not only reduces the base pressure ($p \approx 2 \times 10^{-10}$ mbar), but modifies the residual gas composition so that hydrogen becomes the dominant species. Hydrogen will not significantly stick on the cold surface of the mirror and, for our discussion, is therefore of no or little concern.

Partial pressures inside a system which is not baked but is largely pumped by a cryosystem (being composed by cryopumps or cryopanels) requires a separate analysis. Each system will behave according to their specific design, but one can expect that the partial pressures of gases like H_2O, CO, CO_2, N_2, etc., will be more similar to the ones in a well-baked vessel than in an unbaked one. In UHV chambers with such a diffused cryopump system, we may expect that the total pressure will be dominated by hydrogen, and other gases will each contribute only some percent to it. This simple reasoning suggests that, more than the total pressure, one needs to carefully consider partial pressures of all the gas species that can be cryosorbed on the mirror surface and evaluate the time it will take to develop a detrimental overlayer.

In the following, to give some quantitative estimation, we refer to the case discussed by Hasegawa and co-workers [16], in which H_2O molecules are found to be the main species in the residual vacuum. The amount and type of contaminant gases that can stick to the mirror surface will be specific to the detailed and cryogenic design and history of its vacuum vessel. The considerations we will do, taking H_2O as an example, are general and can be applied also for gases different from H_2O (CO, CO_2, N_2, etc., or a mixture of all).

D. Cryosorbed adlayer thickness

Clearly, a Monte Carlo approach based on detailed surface-molecule energetics and interaction properties will produce accurate results. On the other hand, conservative estimates are required when designing, with some margins, the complex vacuum system hosting the cryogenically cooled mirror for gravitational interferometers. It is, therefore, useful to introduce the Langmuir (L) as the gas exposure of a surface (or dosage), as it is typically used in UHV surface physics to study gas adsorption [28]. It is a practical unit, not dimensionally homogeneous, and it is used only in this one field. The Langmuir is defined by multiplying the pressure of the gas (in Torr) by the exposure time, so that

$$1\ \mathrm{L} = 10^{-6}\ \mathrm{Torr} \cdot 1\ \mathrm{s}. \tag{2}$$

Clearly, surface gas exposure measures the fluence (Φ), with respect to exposed time (t), to a given number of particles per unit area and time (J):

$$\Phi = \int J \cdot dt. \tag{3}$$

The number of gas molecules passing through a surface of unit area in unit time (J) can be derived from kinetic theory:

$$J = \frac{n\bar{v}}{4}, \tag{4}$$

where n is the density of the gas and $\bar{v}$ is the mean speed of the gas particles, given by

$$n = \frac{p}{kT} \quad \text{and} \quad \bar{v} = \sqrt{\frac{8kT}{\pi m}}, \tag{5}$$

respectively, where m is the mass of a given atom (or molecule) composing the gas. Then, putting Eq. (5) in Eq. (4), one obtains

$$J = p\sqrt{\frac{1}{2\pi kTm}}. \tag{6}$$

As seen when discussing the relation between the pressure measured in a room temperature system connected to a cryogenic one, from Eq. (6) it is clear that the proportionality between this flux and the pressure is strictly valid only for a given temperature T and a given gas mass (m) and depends on their square roots. Assuming the pressure in the cold environment as the one corrected by the "thermal transpiration" effect and the fact that we mainly consider light gases forming the residual vacuum, the Langmuir

remains useful as a practical unit for our purposes. Assuming that every gas molecule hitting the surface sticks to it (that is, the sticking coefficient is 1), one Langmuir (1 L) leads to a coverage of about one monolayer of the adsorbed gas molecules on the surface [28]. In general, the sticking coefficient varies depending on the temperature and on reactivity between surface and gas particles, so that the Langmuir gives a lower limit of the time it needs to completely cover a surface with a monolayer.

To give an example of a quantitative estimate, let us consider the case of the test system used in Ref. [16]. In that work, the authors report that the cryogenic mirror is held at 47 K, the thermal screens are held at 80 K, and the final total pressure (measured in a room temperature section) is 6.9×10^{-6} Pa ($1\ \text{Pa} \approx 7.5 \times 10^{-3}$ Torr; $1\ \text{Pa} = 10^{-2}$ mbar). Monitoring the components of residual molecules by a mass spectrometer, they found that the main detected molecules were H_2O, O, and OH, where O and OH can be generated from H_2O. From this information, to evaluate the effective contribution of the mirror vacuum vessel to the H_2O ice growth, we have first considered that the pressure in the cryogenic region close to the mirror surface can be derived by applying the thermal transpiration correction to the pressure measured at room temperature [Eq. 1]. Assuming that the temperature in the region close to the mirror is between the temperature of the mirror (47 K) and of the one of the thermal screen (80 K), we will consider here a thermal transpiration correction of ≈ 2. By doing so, a pressure of $\approx 3.5 \times 10^{-6}$ Pa can be assumed near the cryogenic mirror surface. Moreover, it is reasonable to assume that in this unbaked system, with a significant cryopumping action given by the thermal shields, the relative content of H_2O is only a few percent of the total pressure (suppose here, for example, of the order of 20%). This estimate is the most prone to errors (up to orders of magnitude) and should be taken with great caution. It suggests the importance of a detailed knowledge of partial as well as total pressure to perform the vacuum considerations here reported. All that said, the mirror surface is supposedly exposed to something like 5×10^{-8} Pa of H_2O molecules, corresponding to $\approx 4 \times 10^{-4}$ L/s. This means that in ≈2500 s a monolayer (ML) of water ice will develop on the surface. One ML of H_2O, depending on the growth mode and structure, can be assumed to be ≈0.27 nm thick [29]. This simple reasoning suggests that in a day a ≈9-nm-thick H_2O ice layer will form on the KAGRA test cryogenic mirror held at 47 K in the vacuum conditions as here indicated. Needless to say, if the water content is in reality 10 times lower (or higher) than the one here assumed, the corresponding ice layer will grow with a rate of ≈1 nm/day (≈100 nm/day). We stress here that this estimate, and the method to obtain it, is given for a water ice layer. Clearly, it applies to all gases (CO, CO_2, N_2, etc.) that have desorption temperatures higher than 10 K (see Fig. 1). The aforementioned estimates are based on the strong (but conservative) assumption of a sticking coefficient equal to one and on the total absence of any concomitant desorption mechanism.

From this reasoning, we can finally set new limits for the base operating vacuum in the ET LF tower: A base H_2O partial pressure of $\lesssim 1 \times 10^{-9}$ Pa ($\lesssim 1 \times 10^{-11}$ mbar) is necessary to limit the growth of the ice layer below 100 nm during a full year of operation. Of course, this implies that the H_2O partial pressure should be below this limit also during mirror cooldown. Once the mirror goes below ≈125 K, it will start to adsorb water, and, for this reason, its partial pressure should be already below the set limit. This will imply some extra care in operating the vacuum and the cryogenic system, since they need to be operated in a coordinated way.

E. Other contributions to adlayer formation

As correctly mentioned in Ref. [16], a significant contribution to the gas that will be seen by the mirror surface comes from the room temperature beam pipe, where the laser beam travels. They evaluate the molecular accumulation rate by MOLFLOW+, a Monte Carlo simulator package developed by Kersevan and Ady at CERN [30]. Their calculation results in an estimate of the layer formation rate (η) of 42 nm per day. This should add up to the rate of the residual gas in the UHV chamber, as computed in the previous section, and the overall estimate will result about 2 times higher than the value experimentally observed by the authors. This may be due to the various approximations required for the calculations but also to the concomitant presence of desorption processes, which are not yet considered. Monte Carlo simulations are the correct way to simulate such a contribution to the gas adlayer on cryocooled mirrors, and an increased simulation activity in this direction is certainly expected as activity grows for the various third-generation antenna design studies.

III. MITIGATION STRATEGIES

The problem of adlayer growth on mirrors is certainly a serious issue, and a great effort will be required to limit the causes of its formation as much as possible. Here, we briefly discuss the global compatibility of all the vacuum processes and potential solutions with the maintenance of the very complex structure, suspensions, and devices all contained in an ∼10 m^3 vacuum tank. Passive methods aim to prevent cryoadsorbtion. Reducing the pressure in the UHV chamber containing the mirrors (called "the tower") is, by itself, a great technological (and economic) challenge. The same can be said for the design of the cold to warm vacuum transition, which is the last part of the otherwise RT beam pipe connecting the beam transfer line to the mirror's vessel. Despite all efforts and investments devoted to this aim, it is necessary to exploit active mitigation methods to cure and remove cryosorbed layers

to avoid the need to warm up the mirrors for inducing gas thermal desorption. It seems impossible, in fact, to design a cooling system for a suspended cold mass that would allow a fast temperature cycling. Any mirror warm-up cycle will require a long down time period, reducing, in an unacceptable way, the operational periods of the observatories. As an example, just cooling down the mirrors in KAGRA from 200 K to the foreseen low temperature takes about 1 month [31]. Also, any wise design should consider eventual malfunctioning and cure eventual minor vacuum issues, such as unwanted small leaks, trapped volumes, etc. An optimal vacuum design will therefore not solve this issue but only impact on the frequency of intervention. Major actions will need to be undertaken to regularly remove the gas ice developed on cold mirrors.

Active mitigation methods should then be conceived and studied to enable the full exploitation of cryogenic reduction of thermal noise from mirror test masses. Here, we present some of these potential active remedies which indeed will require significant R&D effort in the years to come.

A. Passive strategies: Low pressure in mirror chambers

Passive strategies aim to reduce the pressure in the mirror vacuum chamber and the gas flow from the long room temperature pipes. There is a complex trade-off between the desired low pressure and its costs and feasibility. One should not forget that the UHV mirror chamber could be (as the present ones) vacuum tanks of about 10 m^3. They need to contain a number of very complex mechanical, electronic, and cabling subsystems. Already, present designs face the complexity of placing under vacuum all the required systems and adopting quite complex solutions not all portable to a cryogenic environment.

It is interesting at this stage to give a quick overview of the vacuum solutions adopted so far. At Advanced LIGO, the chambers with horizontal access (HAM) chambers are single volumes. They are pumped with large noble diode ion pumps (≈2000 l/s each) and liquid nitrogen cryopumps. All those pumps are installed between the various HAM chambers. The operating pressure is in the 10^{-9} mbar range. Virgo mirror chambers, shown in Fig. 3, are also large vacuum tanks of about 10 m^3 and grant UHV around the mirrors with a different approach. At variance with LIGO, mirror chambers at Virgo cannot be heated with the optics installed and have the particularity of having two vacuum compartments, as shown in Fig. 4. The upper one contains the superattenuator mechanics and is maintained at pressures in the range of 10^{-7} mbar. The lower one, containing the mirror, can be operated at $\approx 10^{-9}$ mbar. The compartments are separated by a small tube through which the 15-mm-diameter steel wire of the suspension surrounded by several tenths of electric conductors passes. The small tube has the function of reducing the flow of gas between the two vacuum systems and could

FIG. 3. Photo of some Virgo mirror UHV chambers.

be differentially pumped from a dedicated pumping system. The computed residual conductance will be about 1.8 l/s. Halfway along the tube, a chamber that could be pumped through a soft bellows would allow one to reduce the conductance to about 0.4 l/s.

In reality, future gravitational vacuum chambers (at least the ones containing cryogenic mirrors) will very likely have a design different from the current ones and will, very probably, be even more complex. Cryogenic screens, augmented pump requirements, etc., will need to be hosted

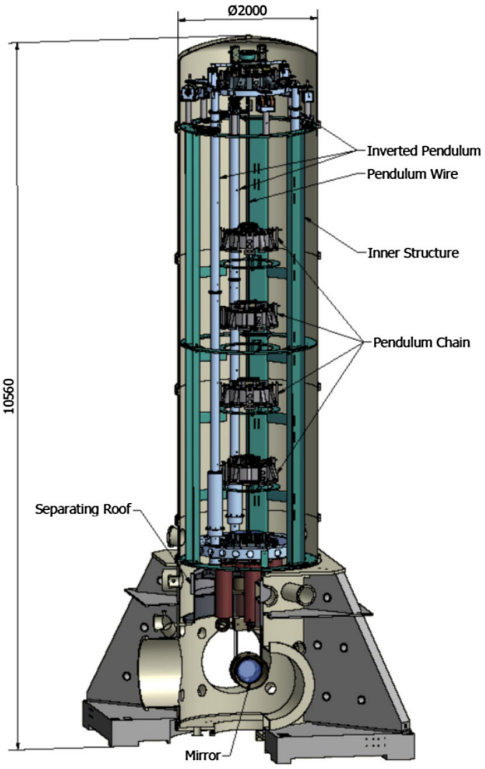

FIG. 4. Drawing of the complex Virgo vacuum system containing the optical elements.

and kept in good vacuum. We do not want here to enter in any details describing solutions that will be the object of future R&D studies. All materials into the vacuum vessels will need to be optimized in preparation and quality, and pumping solutions will have to be validated to be compliant to their many requirements, spanning from affordability to extremely low vibrations, etc.

B. Passive strategies: Low gas flow from beam line

Clearly, one other obvious source of undesired gas impinging on the cold mirror surface is the one traveling along with the laser beam along the entrance beam lines. Such beam lines, as long as 10 km each and large enough to let the laser beam travel without obstacles, have also some stringent vacuum requirements. Vacuum there should be low enough to reduce the noise due to vacuum fluctuations along the beam path to an acceptable level. The ET design study has shown that third-generation interferometers will require to reach in the arm vacuum pipes a total residual pressure of the order of 10^{-10} mbar, corresponding to a noise level of about 10^{-25} $\mathrm{Hz}^{-1/2}$ [11,12]. Even if such vacuum levels are obtained in the arms, all at room temperature, it is essential to decouple as much as possible the RT vacuum with the one of the cryogenic mirror chambers. To this purpose, a so-called "vacuum cold to warm transition" needs to be carefully designed. It has to be long enough to limit the direct molecular flow from the RT parts to the mirror surface and grant ideally a sticking coefficient close to unity, for all the molecules impinging on its walls. In its definition, Monte Carlo vacuum simulations, such as MOLFLOW [30], will be extremely useful. Clearly, nonevaporable getter (NEG) pumps, low-temperature cryopanels, and the use of porous substances, such as charcoal, carbon, sintered metals [32], or nanostructured porous material, to enhance adsorption probability at higher temperatures than on the flat surface counterpart [21,22] will need to be carefully considered to reduce such unwanted gas flow on the mirror surface.

C. Passive strategies: Primary laser-beam-induced desorption

IR photodesorption is assumed to be mainly thermal and will scale exponentially with the laser power. Laser-induced additional heat load is indeed considered and defines the cryogenic budget to keep the mirror at a constant temperature during data taking. This implies that, if all works well, the mirror surface should not increase its temperature, and no thermal desorption will be associated to the impinging laser beam. One can wonder if any nonthermal desorption does take place. This phenomenon, if occurring at all, can be considered as a passive method, since it will always be in place during data taking. There are only a few studies of "true" IR photodesorption [33–36]. One can, in principle, induce nonthermal desorption by IR photons by exciting specific vibration modes of the adsorbate and/or the surface-adsorbate bond. However, while IR-induced thermal desorption (LITD) increases exponentially with laser power, nonthermal mechanisms increase only linearly or quadratically and are quickly drowned out by the LITD signal. Furthermore, in this regime it may be difficult to clearly disentangle between what is "thermal" and "nonthermal." This phenomenon may result to be irrelevant to reduce ice buildups during data taking. Still, it may be worth addressing this issue with some specific experiments to finally quantify the issue for the power, photon energy, temperature, gas composition, etc., specific to the ET detector.

D. Active strategies

In this subsection, we analyze what could be actively done to reduce or remove such gas ices which will inevitably form on the cryogenic mirrors.

E. Active strategies: CO_2 laser

One possible way to solve this problem [17] is to illuminate the cryogenic mirror with a CO_2 laser in the same manner as the thermal compensation system implemented in aLIGO [37]. By CO_2 laser irradiation, the adsorbed molecules will obtain kinetic energy and can desorb from the mirror surface. This laser desorption system heats up only the test mass, and the recooling period should be significantly improved. Still, raising the surface temperature above $\approx$125 K (the necessary temperature to desorb water ices at the pressures in use) with CO_2 laser light will certainly induce some significant heat ups of the cold mass, extra thermal desorption, and thermal flow must be carefully studied to assess the speed of the entire process, given the high thermal conductance of the payload and the limited cooling capacity. Also, the required CO_2 laser power must be carefully tailored to this need. Moreover, since photons will penetrate deep in the surface, the effect of high-power photons on mirror quality must be carefully addressed, since one needs to avoid that defects or color centers in the optical coatings may form, detrimentally influencing mirror optical quality. Therefore, the effect on mirror quality of high-power photons emitted by the CO_2 laser needs to be carefully studied. One other important aspect not to be underestimated is the fact that any temperature-measuring diode directly connected to the mirror (and close to its surface) may induce additional noise and should be avoided. It is not yet clear how temperature will be measured on the optical elements and how this lack of information may affect the CO_2 laser light irradiation times.

F. Active strategies: UV photons

UV photons can stimulate electronic transitions in molecular ice. Once stimulated, these electronic excitations can follow different relaxation pathways, one being molecular desorption but also surface and/or bulk

chemistry and vibration and/or phonon excitation (which can stimulate desorption, also). UV light can therefore induce nonthermal desorption by delivering to the ice enough energy to break physisorption bonds. Therefore, UV photodesorption could be a viable solution to remove ice layers from the cryogenic mirrors. The efficiency of this process is determined by the specific molecular ice and by the radiation energy. Other than the understanding of the physics underlying the desorption mechanisms, the determination of the efficiency of UV photon desorption is of paramount importance. This key parameter is usually called photon stimulated desorption (PSD) and is defined as the number of desorbed molecules per incident photon:

$$\mathrm{PSD} = \frac{N_{\mathrm{mol}}}{N_{\mathrm{ph}}}. \tag{7}$$

PSD for H_2O under UV irradiation has been measured by different research groups (a list of some results can be found in Ref. [38]). Water ice PSD is, in fact, strongly dependent on the specific electronic excited state and on temperature, which, in turn, determines the morphology of ice, compact or porous, amorphous or crystalline. In the study conducted by Cruz-Diaz *et al.* [38], the H_2O yield is 1.3×10^{-3} molecules per photon, for ice condensed at 8 K, and 2.5×10^{-3} molecules per photon, for water ice held at 100 K. The irradiation source in that experiment was a laboratory standard microwave discharged hydrogen flow lamp, covering the 120–165 nm range (10.33–7.51 eV), where H_2O ice shows absorption transitions [39].

Let us go back to the exemplary KAGRA case. We want to roughly estimate the time necessary to desorb the amount of water ice condensed after one day on the cryogenic mirrors in the vacuum conditions described before, considering a typical UV photon flux of $\Phi \approx 2 \times 10^{14}$ photons $\mathrm{cm}^{-2}\,\mathrm{s}^{-1}$ as in Ref. [38]. A H_2O layer of ≈9 nm will be condensed on the mirror in a day. This corresponds to ≈30 ML, that is, a molecule density $n_{\mathrm{mol}} \approx 30 \times 10^{15}$ molecules per cm^2 ($\approx 1 \times 10^{15}$ molecules per cm^2 being the surface density of water ice). By using Eq. (7), the time to let the desorption of such water ice can be estimated as $t = n_{\mathrm{mol}}/(\mathrm{PSD} \cdot \Phi)$. At $T = 47$ K, $\mathrm{PSD} \sim 1.6 \times 10^{-3}$, and then $t \sim 93750$ s. This means that, to remove the water ice condensed in one day on a portion of the mirror area of 1 cm^2, more than one day is required (∼26 h), at least at these irradiation conditions. Of course, one could think to increase the UV photon flux to faster remove water contamination from cryogenic mirrors. However, some more considerations have to be done on the effects of UV irradiation on mirrors. UV photons will easily travel through the ice overlayer and reach the underlaying optical surface. When the incident UV beam of intensity I_i reaches the ice on top of the mirror, part of this intensity (I_{abs}) will be absorbed, causing some desorption, and part of it (I_t) will be transmitted to the substrate in accordance with the Beer-Lambert law:

$$I_t = I_i e^{-\sigma \cdot n_{\mathrm{mol}}}, \tag{8}$$

where σ is the ice absorption cross section. For condensed H_2O, an average σ value of $\approx 3.4 \times 10^{-18}$ cm^2 has been experimentally obtained in the vacuum ultraviolet (VUV) spectral region [40]. If $n_{\mathrm{mol}} \approx 30 \times 10^{15}$ molecules per cm^2, then one will have that $\sigma \cdot n_{\mathrm{mol}} \approx 0.1$. From Eq. (8), this means that the water ice is optically thin in respect to VUV radiation and ≈90% of the incident radiation is transmitted to the mirror.

Although H_2O molecules dominate the residual vacuum composition, other species such as CO and CH_4 inevitably are present as contaminants physisorbed on the cryogenic mirrors. High-energy photons can promote reduction and oxidation reactions of carbonaceous compounds, thus leading to the darkening of parts of the mirrors' surface and compromising their optical quality [41]. Even if morphological modifications of the surface are not induced by UV irradiation at low flux (as, for example, laser ablation or lithography do), some issues could come by the absorption of light. In the case of ET LF, crystalline silicon mirrors are foreseen having a coating to properly reflect the laser light [42]. Among different solutions for material coating, amorphous silicon (a-Si) [43] or HfO_2 doped with SiO_2 have been recently proposed, this latter ideally suiting as a low-index partner material for use with a-Si in the lower part of a multimaterial coating [44]. VUV radiation could be adsorbed and released as thermal energy, thus contributing to the thermal load of cryogenic optics [45]. UV radiation, moreover, could also induce both interface and bulk defects formation, thus modifying the optical properties of mirrors [46,47]. All these aspects should be carefully studied and evaluated, looking at the right conditions and balancing pros and cons in using UV irradiation as an active strategy to remove ice on cryogenic mirrors.

G. Active strategies: Electrons

Electrons are well known to be able to efficiently remove contaminant ice layers [48]. Their use in the GW detector context was never taken into serious consideration, since they will inevitably induce detrimental mirror charging. Such unwanted charging needs to be taken into great account, since it affects the overall efficiency of GW detectors [49,50]. This effect is indeed more significant in interferometers where electrostatic damping is used, as in LIGO [50–52]. In Virgo, where inductive damping is in action [53], the detrimental effects of such electrostatic charging on the test mass has not been observed to be clearly limiting sensitivity up to present performances [54]. Yet, also in those systems, it is unclear if such phenomena could become an issue when sensitivity is pushed to lower limits. Within the LIGO Collaboration, a mitigation method has been proposed and successfully applied [49,55–58]. This method implies mirror long exposure (≈1 h) to some tenth of a millibar of N_2 plasma. This plasma is then

introduced into the tower containing the mirror test masses until neutralization occurs. This mitigation method is inapplicable at cryogenic temperature, since, as discussed for H_2O, a significant layer of N_2 will be cryosorbed on the mirror surface [23], dramatically influencing reflectivity and adding further contribution to the thermal noise. Very recently, rather than using N_2 plasma, it has been proposed that electrons of different energy can induce (or mitigate) charges of both signs [59]. Very low-energy electrons (≈5–10 eV) will deposit a negative charge on the mirror, compensating positive space charge. Slightly higher energy electrons (≈50–200 eV) will extract electrons from the surface, compensating negative space charge. If this method is proved to be applicable in real GW detectors, it opens the possibility of using electrons also to mitigate ice growth on mirror surfaces. Electrons could be used in a synergic tandem both to mitigate charging issues on mirrors and to defrost it without charging it. Having access to electrons for removing ice from mirror surface has, in fact, some advantages: (i) Electrons efficiently induce molecular ice nonthermal desorption [48]. (ii) Low-energy electrons are expected to be extremely mild to the optical surfaces. Electrons do not significantly penetrate into the mirror surface due to their low mean free path, so that minimal effects on mirror quality are expected. (iii) Electron guns are commercially available, can be stably placed and immediately operated in UHV, and are compatible with cryogenic environments. All these can allow short shutdown periods to cure charging and frost growing and can notably reduce cost for vacuum and cryogenic maintenance. The possibility to use electrons also to mitigate ice growth is, therefore, very appealing and will be discussed more in detail in the following.

When electrons with energy in the sub-keV range penetrate into a surface covered with a cryosorbed ice layer, they interact with the molecules through inelastic collisions. Losing energy, they can cause electronic excitations and molecule ionizations. Then, with an initial process similar to UV photons (electronic transitions), impinging electrons can induce molecular ice desorption. In analogy with PSD, the efficiency of electron stimulated desorption (ESD) is given by the electron desorption yield (η_e), defined as the ratio between the number of desorbed molecules and the number of incident electrons (N_{el}):

$$\eta_e = N_{\mathrm{mol}}/N_{el}. \tag{9}$$

The extent of such a parameter is determined by the specific interactions triggered by electrons inside the ice, which, in turn, are governed by the stopping power of target system. The stopping power describes the energy loss per unit distance, by a fast charged particle going through a given material. It depends on the mass, velocity, and charge of the particle as well as on the properties of the material. In addition to the stopping power, η_e depends also on the electron transport mechanisms that define which layers of the ice can be involved in desorption [48]. Electron desorption processes are occurring at the very surface, and electrons penetrate ∼10–15 ML, corresponding to a depth of the order of ∼3–5 nm. This is also the typical escape depth of secondary electrons, always present as the results of the electron interaction in any material. The flow of electrons inside a material is, in fact, governed by the universal mean free path curve [28,60], indicating that electrons (depending on their energy) can move in a very limited distance ranging from up to ∼1 nm (for electrons with energy between ∼10 and ∼1000 eV) or up to ∼10 nm (for electrons having energy less than ∼10 eV or greater than ∼1000 eV). The transport of secondary electrons is, therefore, the principal mechanism governing ESD, and electrons very poorly penetrate inside the substrate. Other transport mechanisms can also contribute, such as excitons and/or diffusion of products chemically induced by electron processing of molecular ice, but both processes are anyway affecting the very top few layers [48,61–63].

Concerning H_2O, Dupuy *et al.* [48] have reported an extensive ESD study on water ice in the multilayer regime (100 ML) as a function of irradiation energy, between 150 and 2000 eV. As reported in Fig. 5(a), the maximum ESD yield ($\eta_e \approx 0.12$) is observed at ∼200 eV. The ice morphology does not significantly affect the desorption of H_2O. Moreover, since desorption will take place only from the topmost few layers, any multilayer thicker than 10 ML (≈3 nm) will behave very similarly to the 100 ML coating shown in Fig. 5(a). Lower coverages, of no interest in the

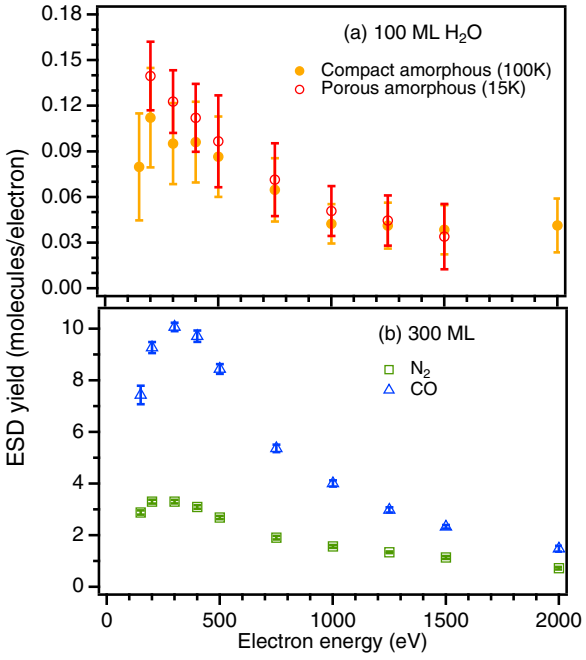

FIG. 5. ESD yield curves from (a) 100 ML of H_2O ice at two different phases and irradiation temperatures and (b) 300 ML of N_2 and CO ices deposited at 14 K [48]. Courtesy of R. Dupuy.

present work, will reflect the interaction of the forming ice with the substrate, and their desorption may differ from the one observed on thick layers here discussed.

In respect to UV photons (PSD $\sim 10^{-3}$), electrons are much more efficient in inducing water desorption. From Fig. 5(a), we can assume an ESD yield of the order of 0.1 H_2O molecules per incident electron at ≈100 eV. Commercially available flood guns can operate with electron current ranging from a few nA to ≈20 mA, in a spot of diameter (d) ranging from ≈10 μm to ≈50 cm. If, for example, 20 mA/cm^2 of electrons at 100 eV (corresponding to 1.2×10^{17} electrons per s cm^2) are delivered on an H_2O layer of about 100 nm thick (≈10^{17} molecules per cm^2), the desorption process will take just about 10 s/cm^2. In the case of ET mirrors (d ≈ 45 cm), defrost would take about 5 h without breaking vacuum. The use of high current, however, has to be carefully evaluated to understand the impact on the thermal budget. With an incident current of 20 mA/cm^2, the power deposited will be no more than 2 W, well above the ET extractable heat power (100 mW) [11–13]. Assuming that all the incident energy is released into thermal energy, to remain below such a thermal budget, a current of at most ≈1 mA/cm^2 should be delivered. In this case, defrost would take about 160 s/cm^2 (≈3 days for the whole mirror). Gain a reasonably fast defrost without dramatically increasing the thermal budget is necessary. On this aspect, however, some considerations can be done by looking at the nature of the desorption process. ESD is a nonthermal mechanism. This means that the energy released by the incident electrons is used to stimulate electronic transitions leading to the breaking of adsorbate bonds and its release. Of course, phonon modes can be also excited, thus leading to a temperature increase. The actual percentage of thermal, desorbing, reflected, etc., energy needs to be evaluated in detail. Anyway, in respect to thermal desorption processes (as by heating with CO_2 laser irradiation), the thermal power deposited on the surface by ESD will be significantly lower. To thermally desorb water, the mirror surface needs to be heated at least above ≈125 K. Once desorption is completed, the mirror needs to be cooled again to 10 K. Presently, it is difficult to estimate how long this process will take, but it could result in an unacceptably long period. Analogously, in the absence of a detailed design, it is difficult to forecast the temperature that will be reached by the mirror during ESD. Indeed, it is safe to assume that the temperature will be much less than 125 K and the time to cool down much faster. At this stage, all these are speculative considerations, and the study of thermal variations induced by electrons is a mandatory task to validate the compliance of the proposed defrost method with the operative constraints. One more issue to be considered is the possibility of irradiating with electrons during data taking. Great care must be used not to induce additional noise to GW detection.

We highlight here that the proposed ESD method to mitigate the frost formation on the mirrors is actually not specific to the H_2O ice layer. Indeed, whatever the gas species condensed on a surface (pure gas or a mixture of gases), the interaction of electrons with the ice does induce desorption, with an efficiency that depends on electron energy and on the ice composition. As an additional example, Fig. 5(b) shows the desorption yield of 300 ML of N_2 and CO as a function of the incident electron energy. More details on these results are given in Ref. [48]. Actually, ESD of both species is even more efficient than for H_2O (for electrons at 100 eV, a factor ≈300 for N_2 and ≈700 for CO). This means that, with the same reasoning so far done for water, an impressive reduction of the time necessary to remove the frost from the ET mirror would be obtained if N_2, or even more CO, is the main residual gas component in the mirror tower. This further example makes evident that also the ESD parameters to be used to remove the frost on the mirrors has to be adapted to the specific vacuum design.

As previously mentioned for photons, electrons can also interact with other residual species foreseen to compose the contamination and could promote their processing through irradiation-induced chemistry [48,60,63,64]. However, these mechanisms are not particularly efficient, especially at low impinging energy [60,64]. Even if unavoidable, the optics darkening problem could be therefore limited. As said, electrons penetrate materials much less than photons, due to their very reduced mean free path. During desorption of most of the water ice, no electrons (neither primary nor secondary) are supposed to reach the mirror surface. Only when electrons erode almost the ice total thickness could they then reach the surface mirror. For ET LF, an optical coating thickness of the order of a few microns is foreseen, which is much higher in respect to the mean free path of electrons in materials. No electrons should be reaching the silicon substrate. The interaction between electrons and the coating layer should be studied and addressed to understand if detrimental effects could arise (for example, at the interface between layers) potentially affecting the optical quality of reflective coating. However, since the thickness of each layer in the coating is more than ≈100 nm, one could expect no defect formation at the multilayer interfaces. The formation of defects could be possible only on the very surface of the mirror coating. The investigation of the effects induced on the coating by electrons is mandatory to determine the compatibility of ESD with the preservation of the mirror optical quality.

IV. CONCLUSION

Here, we have presented a survey of some of the vacuum challenges that will be encountered when designing the new generation of GW detectors. Particular emphasis is given to the analysis of the vacuum system hosting the cryogenically cooled mirrors for the low-frequency detection of GWs. Ice formation can be reduced by design but

cannot be completely eliminated. Frost on mirror surfaces will induce various detrimental effects on mirror optical properties, adsorption, additional thermal noise, etc. This analysis set new limits for an acceptable operating pressure to avoid ice formation in a given period of continuous data taking.

An overview on possible passive and active methods to mitigate such ice formation is then given, analyzing possible advantages, disadvantages, and future R&D research directions. Here, we also propose, for the first time in this context, the use of low-energy (below 200 eV) electrons to efficiently desorb cryosorbed molecules. Electrons are known to be very efficient in nonthermal desorbing condensed molecules from cold surface, to interact only with the topmost layers and, hence, to have a potentially very low impact on optical mirror quality and on deposited heat load. The detailed study of their interaction with a mirror surface could bring about a very important and conceptually simple method that could be applied to eliminate cryogenically formed ice on optical elements in gravitational wave interferometers. Its actual refinement and implementation on the real system is indeed a challenge and will involve specific R&D on many specific issues, including the detailed surface characterization of representative mirror surfaces; design and optimization of newly developed or existing electron guns (or flood guns) and of their mountings; study the effect, if any, of such very low-energy electrons on the optical properties of the mirrors; and the realization of a realistic mock-up system to test the process.

ACKNOWLEDGMENTS

The authors thank B. Barish for enlightening discussions. We thank R. Dupuy and V. Baglin for sharing their ESD source data.

[1] B. P. Abbott, R. Abbott, T. D. Abbott, M. R. Abernathy, F. Acernese, K. Ackley, C. Adams, T. Adams, P. Addesso, R. X. Adhikari *et al.* (LIGO Scientific and Virgo Collaborations), Phys. Rev. Lett. **116**, 061102 (2016).

[2] B. P. Abbott, R. Abbott, T. D. Abbott, F. Acernese, K. Ackley, C. Adams, T. Adams, P. Addesso, R. X. Adhikari, V. B. Adya *et al.* (LIGO Scientific and Virgo Collaborations), Phys. Rev. Lett. **119**, 161101 (2017).

[3] T. Kinugawa, K. Inayoshi, K. Hotokezaka, D. Nakauchi, and T. Nakamura, Mon. Not. R. Astron. Soc. **442**, 2963 (2014).

[4] G. M. Harry, A. M. Gretarsson, P. R. Saulson, S. E. Kittelberger, S. D. Penn, W. J. Startin, S. Rowan, M. M. Fejer, D. R. M. Crooks, G. Cagnoli *et al.*, Classical Quantum Gravity **19**, 897 (2002).

[5] G. M. Harry, M. R. Abernathy, A. E. Becerra-Toledo, H. Armandula, E. Black, K. Dooley, M. Eichenfield, C. Nwabugwu, A. Villar, D. R. M. Crooks *et al.*, Classical Quantum Gravity **24**, 405 (2007).

[6] J. Steinlechner and I. W. Martin, Phys. Rev. Research **1**, 013008 (2019).

[7] P. Amico, L. Bosi, L. Gammaitoni, G. Losurdo, F. Marchesoni, M. Mazzoni, M. Punturo, R. Stanga, A. Toncelli, M. Tonelli *et al.*, Nucl. Instrum. Methods Phys. Res., Sect. A **518**, 240 (2004).

[8] K. Somiya, Classical Quantum Gravity **29**, 124007 (2012).

[9] Y. Aso, Y. Michimura, K. Somiya, M. Ando, O. Miyakawa, T. Sekiguchi, D. Tatsumi, and H. Yamamoto (KAGRA Collaboration), Phys. Rev. D **88**, 043007 (2013).

[10] T. Akutsu, M. Ando, A. Araya, N. Aritomi, H. Asada, Y. Aso, S. Atsuta, K. Awai, M. A. Barton, K. Cannon *et al.*, J. Phys. Conf. Ser. **1342**, 012014 (2019).

[11] M. Abernathy *et al.* (ET Science Team), ET-0106C-10 (2010), https://tds.ego-gw.it/ql/?c=7954(2010).

[12] M. Punturo, M. Abernathy, F. Acernese, B. Allen, N. Andersson, K. Arun, F. Barone, B. Barr, M. Barsuglia, M. Beker *et al.*, Classical Quantum Gravity **27**, 194002 (2010).

[13] S. Hild, Classical Quantum Gravity **29**, 124006 (2012).

[14] D. Reitze, R. X. Adhikari, S. Ballmer, B. Barish, L. Barsotti, G. Billingsley, D. A. Brown, Y. Chen, D. Coyne, R. Eisenstein *et al.*, Bull. Am. Astron. Soc. **51** (2019), https://baas.aas.org/pub/2020n7i035.

[15] S. Miyoki, T. Tomaru, H. Ishitsuka, M. Ohashi, K. Kuroda, D. Tatsumi, T. Uchiyama, T. Suzuki, N. Sato, T. Haruyama *et al.*, Cryogenics **41**, 415 (2001).

[16] K. Hasegawa, T. Akutsu, N. Kimura, Y. Saito, T. Suzuki, T. Tomaru, A. Ueda, and S. Miyoki, Phys. Rev. D **99**, 022003 (2019).

[17] S. Tanioka, K. Hasegawa, and Y. Aso, Phys. Rev. D **102**, 022009 (2020).

[18] V. Baglin, https://cds.cern.ch/record/1047076.

[19] O. Malyshev, *Vacuum in Particle Accelerators: Modelling, Design and Operation of Beam Vacuum Systems* (Wiley, New York, 2019), ISBN 9783527809165.

[20] S. Dushman and J. Laferty, *Scientific Foundations of Vacuum Technique* (John Wiley & Sons, New York, 1962).

[21] L. Spallino, M. Angelucci, R. Larciprete, and R. Cimino, Appl. Phys. Lett. **114**, 153103 (2019).

[22] L. Spallino, M. Angelucci, and R. Cimino, Phys. Rev. Accel. Beams **23**, 063201 (2020).

[23] R. E. Honig and H. O. Hook, RCA Rev. **21**, 360 (1960), https://worldradiohistory.com/RCA_Review_Issue_Key.htm.

[24] T. Takaishi and Y. Sensui, Trans. Faraday Soc. **59**, 2503 (1963),

[25] P. Dawson, *Quadrupole Mass Spectrometry and Its Applications*, AVS Classics in Vacuum Science and Tech-

nology (American Institute of Physics, New York, 1995), ISBN 9781563964558.
[26] H. Schmickler, Technical Report No. CERN-ACC-2020-0009, CERN, Geneva, 2020, https://cds.cern.ch/record/2721872.
[27] G. Bregliozzi, arXiv:2006.10367.
[28] D. P. Woodruff, *Modern Techniques of Surface Science*, 3rd ed. (Cambridge University Press, Cambridge, England, 2016).
[29] U. Bergmann, A. Di Cicco, P. Wernet, E. Principi, P. Glatzel, and A. Nilsson, J. Chem. Phys. **127**, 174504 (2007).
[30] R. Kersevan and M. Ady, in *Proceedings of the 10th International Partile Accelerator Conference (IPAC'19), Melbourne, Australia, 2019* (JACoW, Geneva, Switzerland, 2019), pp. 1327–1330, ISBN 978-3-95450-208-0, https://doi.org/10.18429/JACoW-IPAC2019-TUPMP037, http://jacow.org/ipac2019/papers/tupmp037.pdf.
[31] T. Akutsu, M. Ando, K. Arai, Y. Arai, S. Araki, A. Araya, N. Aritomi, H. Asada, Y. Aso, S. Atsuta *et al.*, Classical Quantum Gravity **36**, 165008 (2019).
[32] C. Day, Colloids Surf. A **187–188**, 187 (2001).
[33] G. Brivio and T. Grimley, Surf. Sci. Rep. **17**, 1 (1993).
[34] I. Hussla, H. Seki, T. J. Chuang, Z. W. Gortel, H. J. Kreuzer, and P. Piercy, Phys. Rev. B **32**, 3489 (1985).
[35] B. Redlich, H. Zacharias, G. Meijer, and G. von Helden, J. Chem. Phys. **124**, 044704 (2006).
[36] C. Focsa, C. Mihesan, M. Ziskind, B. Chazallon, E. Therssen, P. Desgroux, and J. Destombes, J. Phys. Condens. Matter **18**, S1357 (2006).
[37] R. Lawrence, M. Zucker, P. Fritschel, P. Marfuta, and D. Shoemaker, Classical Quantum Gravity **19**, 1803 (2002).
[38] G. A. Cruz-Diaz, R. Martn-Domnech, E. Moreno, G. M. M. Caro, and Y.-J. Chen, Mon. Not. R. Astron. Soc. **474**, 3080 (2018).
[39] K. Kobayashi, J. Phys. Chem. **87**, 4317 (1983).
[40] G. Cruz-Diaz, G. M. Caro, Y.-J. Chen, and T.-S. Yih, Astron. Astrophys. **562**, A119 (2014).
[41] D. Garoli, L. V. Rodriguez De Marcos, J. I. Larruquert, A. J. Corso, R. P. Zaccaria, and M. G. Pelizzo, Appl. Sci. **10**, 7538 (2020).
[42] ET steering committee, technical report, 2020, https://apps.et-gw.eu/tds/ql/?c=15418.
[43] R. Birney, J. Steinlechner, Z. Tornasi, S. MacFoy, D. Vine, A. Bell, D. Gibson, J. Hough, S. Rowan, P. Sortais *et al.*, Phys. Rev. Lett. **121**, 191101 (2018).
[44] K. Craig, J. Steinlechner, P. G. Murray, A. S. Bell, R. Birney, K. Haughian, J. Hough, I. MacLaren, S. Penn, S. Reid *et al.*, Phys. Rev. Lett. **122**, 231102 (2019).
[45] L. V. Rodríguez-de Marcos, J. I. Larruquert, J. A. Méndez, and J. A. Aznárez, Opt. Mater. Express **6**, 3622 (2016).
[46] B. Pivac, M. Pavlović, I. Kovačević, B. Etlinger, and I. Zulim, Vacuum **71**, 135 (2003).
[47] A. Markosyan, R. Route, M. Fejer, D. Patel, and C. Menoni, J. Appl. Phys. **113**, 133104 (2013).
[48] R. Dupuy, M. Haubner, B. Henrist, J.-H. Fillion, and V. Baglin, J. Appl. Phys. **128**, 175304 (2020).
[49] L. G. Prokhorov and V. P. Mitrofanov, Classical Quantum Gravity **27**, 225014 (2010).
[50] A. Buikema, C. Cahillane, G. L. Mansell, C. D. Blair, R. Abbott, C. Adams, R. X. Adhikari, A. Ananyeva, S. Appert, K. Arai *et al.*, Phys. Rev. D **102**, 062003 (2020).
[51] J. Aasi, B. P. Abbott, R. Abbott, T. Abbott, M. R. Abernathy, K. Ackley, C. Adams, T. Adams, P. Addesso, R. X. Adhikari *et al.*, Classical Quantum Gravity **32**, 074001 (2015).
[52] C. Blair, S. Gras, R. Abbott, S. Aston, J. Betzwieser, D. Blair, R. DeRosa, M. Evans, V. Frolov, P. Fritschel *et al.* (LSC Instrument Authors), Phys. Rev. Lett. **118**, 151102 (2017).
[53] F. Acernese, M. Agathos, K. Agatsuma, D. Aisa, N. Allemandou, A. Allocca, J. Amarni, P. Astone, G. Balestri, G. Ballardin *et al.*, Classical Quantum Gravity **32**, 024001 (2015).
[54] F. Acernese, M. Agathos, L. Aiello, A. Allocca, A. Amato, S. Ansoldi, S. Antier, M. Arène, N. Arnaud, S. Ascenzi *et al.* (Virgo Collaboration), Phys. Rev. Lett. **123**, 231108 (2019).
[55] M. Hewitson, K. Danzmann, H. Grote, S. Hild, J. Hough, H. Lck, S. Rowan, J. R. Smith, K. A. Strain, and B. Willke, Classical Quantum Gravity **24**, 6379 (2007).
[56] S. Buchman, R. L. Byer, D. Gill, N. A. Robertson, and K.-X. Sun, Classical Quantum Gravity **25**, 035004 (2008).
[57] P. Campsie, L. Cunningham, M. Hendry, J. Hough, S. Reid, S. Rowan, and G. D. Hammond, Classical Quantum Gravity **28**, 215016 (2011).
[58] D. Ugolini, C. Fitzgerald, I. Rothbarth, and J. Wang, Rev. Sci. Instrum. **85**, 034502 (2014).
[59] M. Angelucci, L. Spallino, R. G. Mazzitelli, Musenich, S. Farinon, A. Chincarini, F. Sorrentino, A. Pasqualetti, G. Gemme, and R. Cimino, Mitigation of the electrostatic charge on test mass mirrors in gravitational wave detectors, in Proceedings of the GWADW2021 Gravitational Wave Advanced Detector Workshop, 2021 (unpublished), https://agenda.infn.it/event/26121/contributions/136341/attachments/81362/106573/GWADW2021_PosterSingle_Angelucci.pdf.
[60] R. Cimino and T. Demma, Int. J. Mod. Phys. A **29**, 1430023 (2014).
[61] J. McConkey, C. Malone, P. Johnson, C. Winstead, V. McKoy, and I. Kanik, Phys. Rep. **466**, 1 (2008).
[62] D. Marchione and M. R. McCoustra, Phys. Chem. Chem. Phys. **18**, 29747 (2016).
[63] M. Bertin, E. C. Fayolle, C. Romanzin, K. I. Öberg, X. Michaut, A. Moudens, L. Philippe, P. Jeseck, H. Linnartz, and J.-H. Fillion, Phys. Chem. Chem. Phys. **14**, 9929 (2012).
[64] R. Cimino, M. Commisso, D. R. Grosso, T. Demma, V. Baglin, R. Flammini, and R. Larciprete, Phys. Rev. Lett. **109**, 064801 (2012).